Partial decoherence and thermalization through time-domain ergodicity

Robert Englman[1] and Asher Yahalom[2,3]
[1]*Soreq NRC, Yavne 81800, Israel*
[2]*Isaac Newton Institute for Mathematical Sciences, 20 Clarkson Road, Cambridge CB3 0EH, United Kingdom*
[3]*Ariel University, Ariel 40700, Israel*
(Received 31 January 2013; published 17 May 2013)

An approach, differing from two commonly used methods (the stochastic Schrödinger equation and the master equation) but entrenched in the traditional density matrix formalism, is developed in a semiclassical setting in order to go from the solutions of the time-dependent Schrödinger equation to decohering and thermalized states. This is achieved by utilizing the time ergodicity, rather than the sampling (or ensemble) ergodicity, of physical systems. We introduce the formalism through a study of the Rabi model (a two-level system coupled to an oscillator) and show that our semiclassical version exhibits, both qualitatively and quantitatively, many features of state truncation and equilibration. We then study the time evolution of two qubits in interaction with a bosonic environment, such that the energy scale of one qubit is much larger and that of the other is much smaller than the environment's energy scale. The low-energy qubit decoheres to a mixture, while the high-energy qubit is protected through the adiabatic theorem. However, an interqubit coupling generates an overall decoherence and leads, for some values of the coupling, to long-term revivals in the state occupations.

DOI: 10.1103/PhysRevA.87.052123 PACS number(s): 03.65.Yz, 75.10.Jm, 05.30.−d

I. INTRODUCTION

Safe and reliable manipulation of quantum states (as is envisaged in a quantum computer) depends on the possibility of error-free and stable quantum systems when left alone, except for the inevitable interaction with the environment. The devil is in the decoherence, and numerous works have been devoted to estimating, minimizing, circumventing it or correcting for it [1]. Distinct from the direct approaches to somehow provide remedies for decoherence, several avenues have been explored in which the quantum system maintains coherence due to the Hamiltonian that defines it. One of the earliest works related to the subject is by Kubo [2], in which hints for the approach taken in the present paper can be found. While decoherence and dissipation are terms very close to each other, "dissipationless decoherence" was also considered [3], and decoherence-free subspaces in the Hilbert space were studied in [4]. In more recent works such subspaces were identified, manifesting "partial decoherence," through symmetry-based discrimination between parts of the Hilbert space [5,6].

The present work also treats partial decoherence but differs from the previous works in that, rather than throwing the burden of discrimination on a specially contrived Hamiltonian, it finds discrimination between Hilbert subspaces more generically, through their having different energy scales. A simple physical example of this is an atomic system in the presence of a magnetic field of 1 T, for which the electronic spins separate to about 10 cm^{-1} and the nuclear spins separate to about 10^{-2} cm^{-1}. As already indicated, an allied idea was briefly noted by Kubo [2], who differentiated between the cases of fast and slowly modulated frequencies of the relaxing system. A further idea borrowed in the present work from that paper (and indeed from other treatments involving "ergodicities") is equating ensemble averages with long-time averages [7].

The proposed semiclassical formalism (which is the main point of this work) is introduced and tested in Sec. II on the single qubit (or 1/2 spin)–single boson (Rabi) model [8]. This was thoroughly treated algebraically [9–13] and applicatively: for single trapped ions [14], chiral molecules in a three-level system [15], Josephson junctions [16], a single photon coupled to a superconducting (SC) qubit [17], and the Bloch-Siegert shift in a SC flux qubit [18]; all of these were treated with a somewhat long-term view of decoherence-ridden quantum computing. The case of two qubits, interacting with a single classical oscillator and having largely differing Zeeman splitting energies, is considered in Sec. III and is the essential motivation for this work. The two-qubit case was featured in [19] and was recently treated algebraically in [20] in cases amenable to adiabatic treatment, but when the two qubits have identical splitting energies.

II. DECOHERENCE IN A SEMICLASSICAL RABI MODEL

Here the spin-vibration Hamiltonian

$$H(t,a) = e\sigma_z + k\sigma_x \sin(\omega t + \alpha_a)(\omega \to 1) \qquad (1)$$

describes our two-parameter system, involving a Zeeman-split 1/2 spin [represented by the Pauli matrices $\sigma_z = \left(\begin{smallmatrix}1 & 0\\ 0 & -1\end{smallmatrix}\right)$, $\sigma_x = \left(\begin{smallmatrix}0 & 1\\ 1 & 0\end{smallmatrix}\right)$] and a classical vibrator, whose frequency ω is equated to 1, thus setting the time t scale and the energy scales of the splitting $2e$ and of the spin-vibration coupling k. α_a is an initial phase of the classical vibrator, whose value is specified by the indexing parameter a. The Hamiltonian of the classical vibration is not needed. In our procedure the time-dependent Schrödinger equation (TDSE) $[i\frac{d\psi_a(t)}{dt} = H(t,a)\psi_a(t)]$[1] is solved numerically with some fixed initial conditions.

[1]We use units in which $\hbar = 1$.

A. Programmatic summary of the three steps to construct the density matrix ρ_{mn}

(1) We adopt the von Neumann definition [21–23]:

$$\rho_{mn}(t) = \frac{1}{\left(\sum_a 1\right)} \sum_a \langle m|\psi_a(t)\rangle\langle\psi_a(t)|n\rangle. \tag{2}$$

In this definition the summation index a represents the values of all coordinates, variables, etc., external to the system (e.g., those of the environment affecting the system) and appearing also in the Hamiltonian. Thus the set $\psi_a(t)$ for all a's forms a time-dependent *ensemble* of states. The degrees of freedom of the system are implicit (not written out) in $\psi_a(t)$.

(2) We solve only for a single external condition, thus dispensing with the a index in the wave function but obtain $\rho(t)$ as the average over an adequate set of adjacent times:

$$\rho_{mn}(t) = \frac{1}{2\Delta t} \int_{t-\Delta t}^{t+\Delta t} d\tau \langle m|\psi(\tau)\rangle\langle\psi(\tau)|n\rangle. \tag{3}$$

This should be equivalent to Eq. (2) if the ergodic hypothesis holds for the duration $2\Delta t$. It also represents a considerable simplification in numerics since the TDSE is only solved once, specifically for $\alpha = 0$. To justify the replacement of step 1 by step 2 we note that in all cases considered, numerically computed nondiagonal density matrix elements were several orders of magnitude smaller than the diagonal ones. Thus decoherence, which is the "truncation" of [24], was achieved. The time-averaging method also avoids the notorious "initial slippage" problem [25]. More detailed motivation for step 2 is given in Sec. IV, after the reader has been informed of the proposed method.

(3) For the basis n,m set we have chosen two alternative representations: (a) the spin eigenstates [up: $\binom{1}{0}$ and down:$\binom{0}{1}$] and (b) the time-dependent adiabatic representation, which is given by the two instantaneous solutions $u(t)$ of $H(t,a)u(t) = w(t)u(t)$, with $w(t)$ being the adiabatic energies. While the spin-up and -down representation has been featured in many works (e.g., [9–13]), the broader issue of representation choice in the density matrix has been intensively studied, e.g., in terms of the "einselection" in quantum measurements [26] and for the preference of energy states [27].

Further discussions of these steps are given in the following.

B. The significance of averaging in steps 1 and 2

Clearly, without averaging, the density matrices could be brought to a pure state form, with only one (diagonal) element unity and all the rest being zero. Illustrating this for an $N \times N$ density matrix when $N = 2$, one can write the density matrix in the alternative forms

$$\begin{pmatrix} a^*a & a^*b \\ b^*a & b^*b \end{pmatrix} \equiv \begin{pmatrix} a^* \\ b^* \end{pmatrix} (a \quad b) \tag{4}$$

showing that the two rows are linearly related. Therefore one eigenvalue of the matrix is zero, while the other eigenvalue is, by invariance of the trace,

$$a^*a + b^*b = 1 \tag{5}$$

due to normalization. The density matrix can thus be brought to a form for a pure state. The same procedure holds also for any density matrix of size $N \times N$, with $N > 2$, where the number of linear relations, and therefore of zero eigenvalues, is $N - 1$. It is only when averaging is performed *first* and the diagonalization of the averages is made subsequently that a mixed state can arise and decoherence, with the vanishing of off-diagonal density matrix elements, emerges.

However, to proceed literally as described in step 1, namely, summing the density matrix over all (in practice, say, 1000) initial phases of the oscillators would have meant solving the TDSE 1000 times and saving all these solutions. Instead, as noted in step 2 above, we have solved it only once for one parameter set and averaged all density matrix elements over some time interval $2\Delta t$. This time interval will be specified as we progress, the criterion being that averaging over a greater interval does not alter the value of the averages. The relation of this procedure to ensemble averaging is rooted in the ergodic theorem (or hypothesis) [7]. We have also constantly checked our results for error and found that the full trace of the averaged density matrix deviated from (was short of) unity by less than 4%, although we have extended our computations over about 200 times the vibrational period $(2\pi/\omega)$. Moreover, the normalization check of the wave-propagated wave function was also in error by the same margin (about 4%), indicating that the error in the density matrix has arisen from numerical errors in the forward integration and not from inadequate tracing (averaging).

C. The environment interaction

A widespread formulation of the interaction of a bosonic environment with a spin system is to write the interaction of the spins with one or more oscillators in the form

$$\sum_n \sum_{i=x,y,z} k_n^i q_n \sigma_i, \tag{6}$$

where q_n is the nth oscillator's amplitude and k_n^i is its coupling strength for the interaction with the spin [28,29]. The behavior of the closed (spin-boson) system is studied through its density matrix $\rho_{s,b}$. The reduced density matrix of the spin system ρ_s is then obtained from the trace $\mathrm{Tr}_b\rho_{s,b}$ over all boson states and modes of the environment. What is the relation of this formulation to our model?

In Eq. (1) we have chosen an (Einstein) model for the oscillators, so that their frequencies are the same (denoted by ω and equated to 1). However, the stochastic (random) effect of the environment on the spin systems is still present through each oscillator having a different phase α_a, randomly distributed between 0 and 2π. We then replace the *set* of randomly phased oscillators acting together by an *ensemble* of independently acting oscillators, with each oscillator having a phase α_a, randomly distributed over the ensemble states. Here a enumerates members of the ensemble. In summary, by the adopted semiclassical approximation for our model in Eq. (1), the oscillator amplitudes and coupling strengths in Eq. (6) take the (unnormalized) forms

$$q_a = \sin(\omega_a t + \alpha_a), \quad k^x = k, \quad k^y = k^z = 0, \tag{7}$$

with a labeling different states of the environment. In the von Neumann averaging in Eq. (2), it is the values of α_a that are to be summed over (eventually, integrated). In the sense of

spin-environment perturbation, the sine term represents highly colored noise.

In the next development of the present formalism, noted in the previous section and in step 2 of Sec. II A, the averaging over the solutions with differing initial phases α_a has been replaced by averaging over a time interval $2\Delta t$.

D. Decoherence results

The decohered diagonal matrix elements with time averaging over about five vibration periods and after reaching equilibration (such that longer times do not essentially change the average values and with near-zero off-diagonal matrix elements, not shown) are presented in Figs. 1–4 in the spin representation (long-dashed lines) and in the adiabatic, time-instantaneous state representation (short-dashed lines). In Fig. 1 for weak spin-oscillator coupling ($k \ll 1$) the initial (upper) state's density matrix (mean occupation probability) is close to 1 but then decays to 1/2 as the coupling k increases. The computed lower state's mean occupation probability was found to be 1 *minus* the one shown, correct to about 0.001, verifying the normalization of the density matrix. The limiting value of 1/2 is appropriate for equilibration with an oscillator bath at infinite temperature, which pertains to this model. (Finite temperatures and thermalization are treated in the next section.)

There are sudden jumps here as in the following figures, whose nature is not clear but probably reflect some resonances (i.e., occurrences when the instantaneous energy differences between the states match the oscillator frequency, $\omega = 1$). To discount the time windows as the sources for the peaks (and also to provide assurances for the reliability of the time-averaging procedure), we have consistently checked the accuracy of the averages by varying the time window by 60%–100%. The variations caused changes in the time averages that were comparable to the widths of the lines in our figures. Sharp variations in the state probabilities were also seen for relatively small variations in the parameters of the Hamiltonian in Fig. 9 of [9] (there termed "unusual behavior").

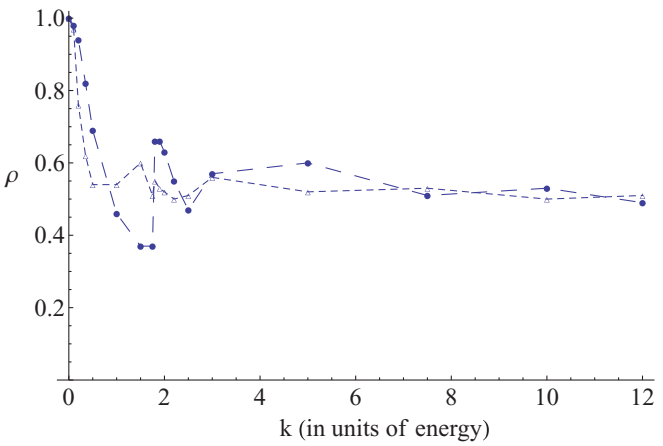

FIG. 1. (Color online) Decohered density matrix elements as functions of the spin-classical oscillator coupling k for low spin energy $e = 0.1$. Dots (connected for visual convenience by long-dashed lines) show spin-up probability. Triangles (connected by short-dashed lines) show upper energy state occupation in the adiabatic energy state representation.

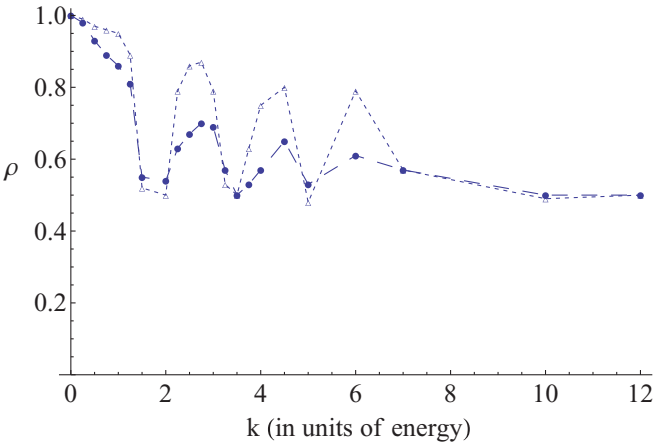

FIG. 2. (Color online) Decohered density matrix elements as functions of coupling strength k for moderate spin energy $e = 1$. Dots: Spin-up probability. Triangles: Upper energy state occupation in the adiabatic energy state representation.

In Fig. 2 the same quantities are shown for spin energy $e = 1$ of the same value as the oscillation frequency. The equilibration starts for larger k and the oscillations (resonances?) are stronger.

Figure 3 is for spin energy $e = 10 \gg 1$ (equal to the vibration frequency ω), representing a situation where the adiabatic theorem holds, so that there is no environment induced mixing of states. As seen, this holds for moderate values of the coupling, but for very strong coupling ($k \gg 1$) the adiabaticity protection breaks down.

Figure 4 shows the inverse situation, where the coupling strength is held fixed at $k = 2.5$ and the spin energy is varied from $e \simeq 0$ (equilibrated case) to a large value (the adiabatically protected regime).

E. Thermalization

While the results in Figs. 1–4 show decoherence at essentially infinite temperature [$T \equiv 1/(k_B\beta) \to \infty$] or with

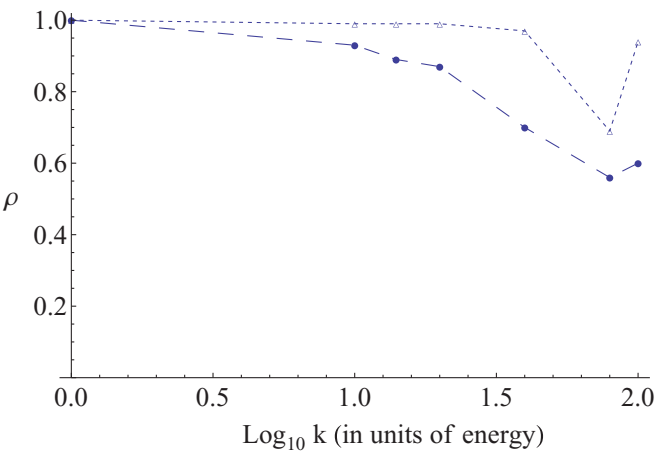

FIG. 3. (Color online) Decohered density matrix vs k in the adiabatically protected spin ($e = 10$) regime. The meaning of the curves is as in Fig. 1. The coupling parameter k reaches only 2; for much larger values the numerical results were not reliable.

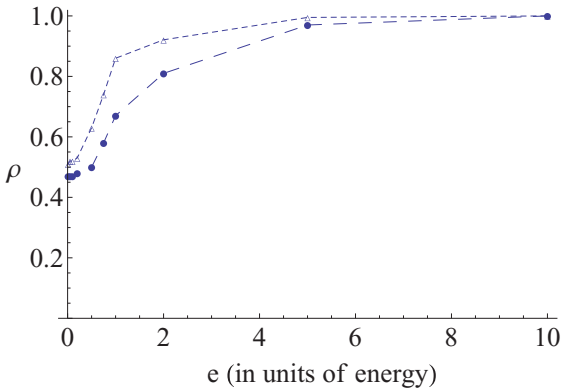

FIG. 4. (Color online) Decohered density matrix plotted against spin energy e for fixed coupling strength ($k = 2.5$). Curves are as in Fig. 1.

the same probability for up and down flipping by the oscillator, at finite temperatures the two probabilities differ. Since in our model stochasticity enters through time averaging, we include temperature effects by weighting the time duration according to the energy of the system, meaning that excursions at lower energies have greater time weights than those at higher energies. Quantitatively, we express Eq. (3) in the adiabatic energy representation, in which $m(t)$ indexes the two states in the adiabatic representation. Then we replace the diagonal terms in Eq. (3) by

$$\rho_{mm}(t) = \frac{1}{2\Delta t}\int_{t-\Delta t}^{t+\Delta t} d\tau \frac{e^{-\beta E_m(\tau)}|\langle m(\tau)|\psi(\tau)\rangle|^2}{\langle\psi(\tau)|e^{-\beta H(\tau)}|\psi(\tau)\rangle} \qquad (8)$$

in which the denominator in the integrand ensures the normalization of the density matrix. The off-diagonal elements are negligible also in the thermalized density matrix.

An intuitive justification for the chosen time weighting can be based on the early work of Rechtman and Penrose [30], who have shown that the probability distribution for a finite classical system in thermal contact with an infinite (in practice, sufficiently large) heat bath, with the composite system being distributed microcanonically, is the Gibbs canonical distribution $e^{-\beta E}$, where E is the energy of the system. This has the meaning that for a state of energy E of the system and no degeneracies, the number of microstates of the heat bath is proportional to $e^{-\beta E}$. If we now suppose that the heat bath spends equal *time* in each microstate (cf. the ergodic hypothesis), then in the system's time integration the infinitesimal dt has to be weighted by the Gibbs factor, as in Eq. (8).

To check the validity of our proposed thermalization procedure, we investigate whether we regain through it the $\rho_{mm} = e^{-\frac{E_m}{k_B T}}/Z$ law. In Fig. 5 we show the logarithm of the ratio of the up and down (time-averaged) diagonal density matrices in the adiabatic state representation, divided by the adiabatic energy difference, against the inverse temperature $\beta \equiv \frac{1}{k_B T}$. In thermalized energy eigenstates the plot should be linear in β with a slope of 1. This is approximately the case for the three lower curves (in which $k \leqslant 1$, weak to moderate spin-oscillator coupling), but for the uppermost curve (in which $k = 2.5$) the spin is too interwoven with the environment to thermalize independently of it.

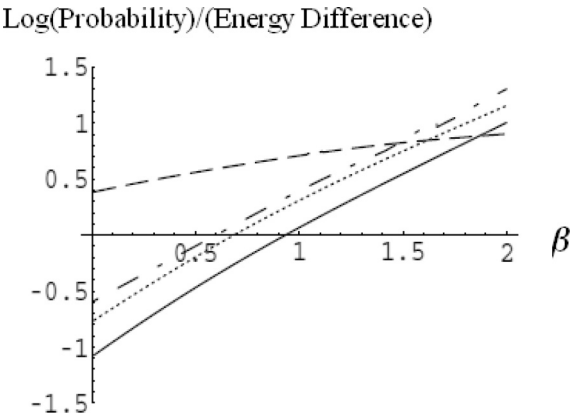

FIG. 5. Thermalized density of states. The input parameters for the curves from bottom to top (at $\beta = 0$ or infinite temperature) are the following: Solid line: spin energy $e = 0.5$, coupling $k = 1$, time*frequency = 270, vertical displacement = 0, (in this curve the mean slope is 1). Dotted line: $e = 0.5$, $k = 1$, time*fr. = 60, vertical displacement = 0.2. Chained line: $e = 5$ (near adiabatic), $k = 0.2$, time*fr. = 250, vertical displacement = 0.6. Long broken line: $e = 0.1$, $k = 2.5$, time*fr. = 250, vertical displacement = 0.4. Curves are displaced vertically for visual clarity.

F. Revivals

To establish the compatibility of our approach with previous works (some of them analytic) on the Rabi model, we turn to a study in which the oscillator state was modeled by a coherent state ([9], Sec. III). As is well known, coherent quantum states resemble closely the behavior of a classical oscillator (which features in our Hamiltonian). Long-period (compared to the oscillator's period) revivals in the spin-up (or spin-down) state probabilities (equivalent to the diagonal terms in the reduced density matrix) were shown in Fig. 7(a) of [9] in the adiabatic limit. The curve computed by us and shown in Fig. 6 (persistent for many further periods, not shown) is extremely similar to their result for a coherent state. Our parameter choice (spin energy $e = 0.05$, spin-oscillator coupling strength $k = 2.5$) is not immediately translatable to that ($\langle N\rangle = 1, \lambda/\omega = 0.1$) in [9] since the coupling strength k in our semiclassical formalism is a combination of these. We have also found that the complete revival pattern shown in Fig. 6 occurs for a restricted choice of parameters and is not a universal feature of the model. However, referring to the Figs. 9(a) to 9(e) of [9], we note that also in their model even slight changes of the parameters cause radical changes in the patterns.

III. TWO-QUBIT SYSTEMS

The Hamiltonian $\mathbf{H}_{\text{total}}(t)$ involves two half-spin systems (qubits), whose parameters are consistently designated by capital and lowercase letters, respectively, interacting with a classical boson source (as before, vibrational or lightlike) varying with time:

$$\mathbf{H}_{\text{total}}(t) = H(t) + h(t) + \mathbf{H}_{\text{int}}, \qquad (9)$$

$$H(t) = E\Sigma_z + K\Sigma_x \sin(\omega t + \alpha), \qquad (10)$$

$$h(t) = e\sigma_z + k\sigma_x \sin(\omega t + \alpha'), \qquad (11)$$

$$\mathbf{H}_{\text{int}} = \gamma(\Sigma_z\sigma_z + \Sigma_x\sigma_x) + \gamma'(\Sigma_x\sigma_x + \Sigma_y\sigma_y), \qquad (12)$$

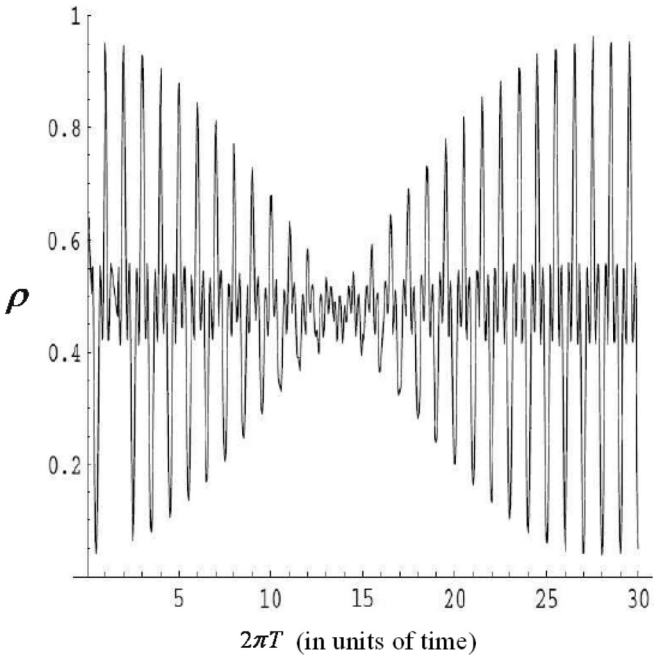

FIG. 6. Time-averaged spin-up probability. Model parameters: spin energy $e = 0.05$, spin-oscillator coupling strength $k = 2.5$, time averaging over $1.2/\omega$, $\omega = 1$.

where the total Hamiltonian (9) comprises Hamiltonians (10) and (11) and Eq. (12) gives the interaction between these. E and e are the energies of the two spin systems, Σ (!) and σ are Pauli matrices operating in the respective spin-spaces, K,k, and α are parameters of the spin-boson couplings, and ω is the frequency of the interacting source. The external boson source is classical, and for it the Hamiltonian need not be written out.

The strengths of the spin-spin interaction are denoted by γ and γ'. For the form of the interaction two alternative submodels will be used: The first, named the two-dimensional model, for which $\gamma \neq 0$ and $\gamma' = 0$, is fashioned after the $E \otimes e$ vibronic interaction [31]. The second, in which $\gamma' \neq 0$ and $\gamma = 0$, is commonly featured in Ising models and is known as the transverse interaction. It has been recently used for superconductors with a large pseudogap and weak long-range Coulomb interaction [32].

The double inequality (exemplified with a physical model in the Introduction)

$$E \gg \hbar\omega \gg e \tag{13}$$

is the keynote of the present section, in that it makes the time variation in the Hamiltonian slow (adiabatic) with respect to that of one of the spins (the one given by capital letter) and fast (nonadiabatic) with respect to that of the other (the one given by lowercase letters). It is therefore expected that the distilled wave function in the former's Hilbert space will stay coherent, while that in the latter's Hilbert space will decohere. This result is indeed found, and some interesting features will be expatiated on in the following. (Two spin systems with *identical* energies were treated in the adiabatic limit in [20].)

We wish to investigate decoherence in the combined system. In an overwhelmingly large number of papers "decoherence," leading from an initially pure to a later mixed state, has been obtained by going from the density of states in the full Hilbert space to that in a partial Hilbert space, through tracing over the complementary Hilbert space (e.g., see references in [24]). As noted earlier in the programmatic summary of Sec. II A, we use an alternative procedure for decoherence, namely, an external parameter averaging procedure. In terms of our model, in which the environment is represented by a classical oscillator, this means that after obtaining a (time-dependent) solution $\psi_{\alpha,\alpha'}(t)$ for given phases α,α', we average the elements of the density matrix $\rho_{nm}(t)$ with respect to all values of these parameters. Then, formally,

$$\rho_{nm}(t) = (4\pi^2)^{-1} \int_0^{2\pi} d\alpha \int_0^{2\pi} d\alpha' \langle n|\psi_{\alpha,\alpha'}(t)\rangle\langle\psi_{\alpha,\alpha'}(t)|m\rangle \tag{14}$$

for some chosen representation, whose components are labeled (n,m). This procedure differs from the commonly used ones (e.g., the stochastic Schrödinger equation or a time-propagation equation for the reduced density matrix) in which the environment is also in a quantum state, whose nature is specified by its spectral properties [33]. Still the method used here is historically primordial (coming from [21,22]). It is also suitable for numerical calculations and alleviates, to some extent, the classical-quantal dichotomy, extensively treated in [24].

The four-component wave function ψ is inserted from the numerical solution of the time-dependent Schrödinger equation (with $\hbar = 1$),

$$i\frac{\partial\psi_{\alpha,\alpha'}(t)}{\partial t} = \mathbf{H}_{\text{total}}(t)\psi_{\alpha,\alpha'}(t), \tag{15}$$

with the appropriate initial condition at $t = 0$. This system is then in a pure state; to track down its progression in interacting with a stochastic environment towards a (possibly) mixed state, we need to consider the density matrix of the system.

As already remarked, the density matrix is representation dependent (although its trace is not), and the choice of the representation (labeled above nm) for the density matrix was extensively discussed in several publications (e.g., [26]). The conclusion there was that an "environment induced selection (einselection)" takes place due to the (experimentalist's) choice of the pointer, which is expressed by the form of the interaction between the environment and the system. In this choice, the off-diagonal matrix elements of the system's density matrix vanish in a time shorter than other time scales in the system's Hamiltonian. (It will be seen that our numerical results support their choice for einselection.) Furthermore, under conditions of weak coupling and large energy scales it was formally shown in [27] that the choice pointer states are the discrete energy states of the system. In this context, one recalls an early, somewhat enigmatic statement in [34]: "In general, only quantities quasi-diagonal in the energy representation are observable."

This has dictated the choice for one of our two adopted representations (representation b in the programmatic summary

in Sec. II A) as the adiabatic solutions of the Hamiltonian, namely, the instantaneous (upper and lower energy) solutions $u(t)$,$l(t)$ for the low-energy part of the Hamiltonian [35], i.e.,

$$h(t)[u(t)/l(t)] = w_{u/l}(t)[u(t)/l(t)], \tag{16}$$

and, likewise, the adiabatic solutions $U(t)$,$L(t)$ for the high-energy part of the Hamiltonian:

$$H(t)[U(t)/L(t)] = W_{U/L}(t)[U(t)/L(t)]. \tag{17}$$

Thus the 4×4 density matrix is written in the representation of Uu,Ul,Lu,Ll in the given order. The appropriate initial condition is an energy eigenstate at $t = 0$. The alternative choice for the representation, namely, the more conventional spin-up and -down representation (representation a in Sec. II A), is not treated in this two-qubit section since we could not find results in the literature to which we might make a comparison.

Actually (as already indicated in Sec. II A), for the sake of simplifications in our procedure, to obtain the density matrix at any time t, we have averaged not over the initial parameters α,α', but rather, with fixed values of $\alpha = 0 = \alpha'$, over a spread of the times $(t - \Delta t, t + \Delta t)$, with Δt being, in the two-qubit case, close to the oscillator period squared, $(2\pi/\omega)^2$, or about 40 in our time units [$\omega = 1$; see the integral in Eq. (14)].

A. Noninteracting spin systems

As a start, we consider the simplified situation in which the spin systems do not interact, i.e., $\gamma = \gamma' = 0$ in Eq. (12). Although this case can be treated for the two spins separately, for the sake of continuity with the interacting spin case in later sections, we treat the two spins as belonging to a larger, combined Hilbert space. We show below the resulting 4×4 density matrix obtained, as described above, from averaging over neighboring times (by an integration over about 10 oscillator periods) and then further representing the obtained averages by their mean values over the full computed time range (in practice about 500 vibrational periods), together with the specification of the standard deviation of the values inside this time range. The obtained results are shown in Fig. 7 for

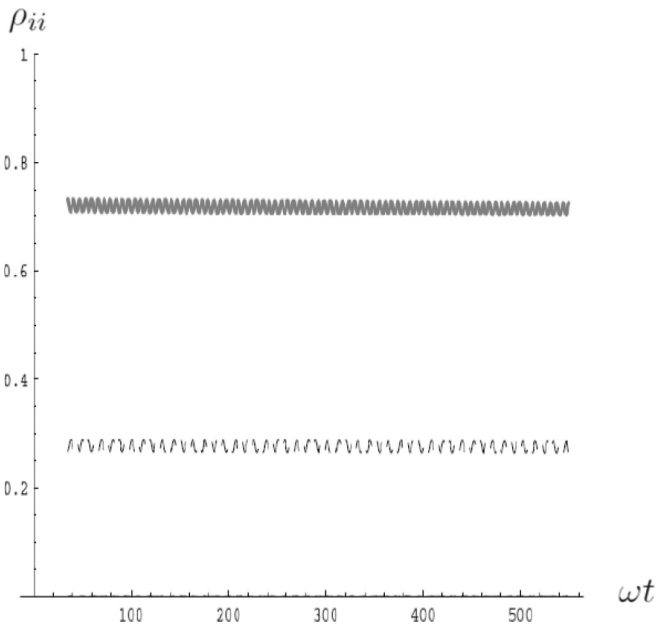

FIG. 7. Diagonal density matrix elements ρ_{ii} ($i = [Uu,Ul,Lu,Ll]$) vs normalized time. Time averages of overlap squares are shown in the adiabatic representation described in the text. Only the diagonal matrix elements for $i = Uu,Ul$ (shown in this order from top to bottom) are visible, while those for $i = Lu,Ll$ are too small to be visible without magnification. Since at any reduced time ωt the averaging spreads over ± 30, the first shown value is above 30, thus missing the starting values for the four-component wave function (1,0,0,0). The constancy of the averages and the small deviations from these throughout the time range should be noted.

the chosen parameter values of

$$E = 5, \quad e = 0.1, \quad K = 2, \quad k = 0.125,$$
$$\alpha = \alpha' = 0, \quad \gamma = \gamma' = 0 \tag{18}$$

in units of ω, which are characteristic of other parameter values.

The time-averaged density matrix is shown next:

$$\langle\rho\rangle = \begin{matrix} \langle Uu| : \\ \langle Ul| : \\ \langle Lu| : \\ \langle Ll| : \end{matrix} \begin{pmatrix} 0.721 \pm 0.015 & 10^{-2} & 10^{-4} & 10^{-4} \\ 10^{-2} & 0.272 \pm 0.010 & 10^{-5} & 10^{-3} \\ 10^{-4} & 10^{-5} & 2 \times 10^{-4} & 10^{-6} \\ 10^{-4} & 10^{-3} & 10^{-6} & 4 \times 10^{-4} \end{pmatrix}. \tag{19}$$

The $\pm$ deviations represent estimated variations in the values over the whole time investigation range. Their signature in Fig. 7 is the small wiggles on the otherwise horizontal lines. The off-diagonal entries show the upper limits to absolute values. The deviations are partly due to computational inaccuracies, partly to the finite range of the averaging process, and partly to the parameters not being in the extreme adiabatic limit.

It may be added that the above error checking refers exclusively to the diagonal terms in the density matrix, whereas the *averaged* off-diagonal matrix elements were unexceptionally negligible. This means that the (adiabatic, instantaneous) representation used here was indeed the proper (einselected) one. These results then lend numerical support for the analytical arguments of Paz and Zurek [27].

1. Reduced density matrices

With the complementary subsystem traced over, the reduced density matrices for the low- and high-energy systems

are (with suppression of errors), respectively,

$$\langle \rho_{u/l} \rangle \approx \begin{matrix} \langle u| : \\ \langle l| : \end{matrix} \begin{pmatrix} 0.721 & 0 \\ 0 & 0.272 \end{pmatrix}, \tag{20}$$

$$\langle \rho_{U/L} \rangle \approx \begin{matrix} \langle U| : \\ \langle L| : \end{matrix} \begin{pmatrix} 0.993 & 0 \\ 0 & 0 \end{pmatrix}. \tag{21}$$

The low-energy system is thus seen to have decohered, or to be in a mixture state (with the partitioning of the weights depending on the values of the parameters, e,ω,k), while the high-energy state is throughout in a coherent, pure state due to its protection by the adiabatic theorem. For situations not belonging to the extreme adiabatic limit (represented by $\frac{E}{\hbar\omega} \longrightarrow \infty$), there will be a finite decoherence time, during the course of which the pure state also decoheres (equilibrates). This decoherence time will decrease as the above ratio decreases, but in our computation range (typically 500 vibrational periods) we have not found for the high-energy (adiabatically protected) states a finite decoherence time.

When the environment coupling to the low-energy system was enlarged to $k = 0.5$ (instead of $k = 0.125$, as in the previous case), the diagonal matrix elements took the *mean* values, with their standard deviation not noted, [0.804,0.192,0.0004,0.0000].

B. Systems with spin-spin interaction

1. Two-dimensional submodel, $\gamma \neq 0, \gamma' = 0$

Weak interaction. We first investigate how the interaction between the spin systems modifies the decoherence discrimination between adiabatic and nonadiabatic systems. In Fig. 8 the diagonal density matrix elements are shown for $|\gamma| \leqslant 1$. Let us set, somewhat arbitrarily, the criterion for decoherence discrimination between high- and low-energy states as a 80% purity for the high-energy states. The thick line in Fig. 8 shows the sum of the two uppermost thin curves (for Uu and Ul): One sees that the >0.8 criterion for purity is well satisfied for negative couplings in the range $0 > \gamma > -1$ but does not hold near the upper values in the positive range $0 < \gamma < 1$, for

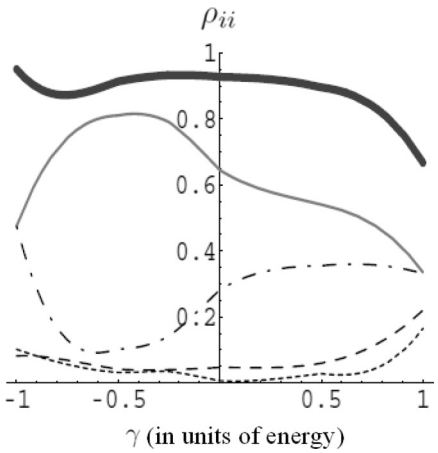

FIG. 8. Diagonal density matrix elements ρ_{ii}, $i = [Uu,Ul,Lu,Ll]$ (for the thin curves in this order from top to bottom), as function of a weak γ (the two-dimensional spin-spin coupling strength). The thick curve is the sum of Uu and Ul, giving the diagonal U term in the reduced density matrix.

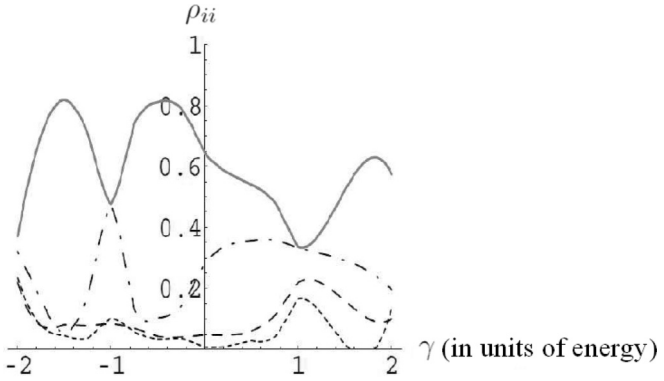

FIG. 9. Diagonal density matrix elements against γ, the two-dimensional spin-spin coupling strength for extended values of the coupling. The meaning of the curves is as in Fig. 8.

which the two curves do not add up to 0.8. One also notices that for $|\gamma| \approx 1$ the low-energy states (u and l) are "fully" mixed, i.e., their diagonal values are equal. However, this does not hold for higher coupling strength, as Fig. 9 illustrates.

Higher interaction strengths. In Fig. 9 one sees that as the coupling strength γ is varied, a high level of weight exchange takes place between the terms, especially between the diagonal Uu and Lu terms. One notes signs of the "level crossing avoidance" phenomenon, familiar from energy level plots for interacting states.

C. Ising coupling model, $\gamma = 0, \gamma' \neq 0$

Numerical results are shown in Fig. 10 (for parameters $E/\omega = 5, e/\omega = 0.1, K/\omega = 4, k/\omega = 2.5$).

1. Remarkable appearance of revivals

"Revivals," or large-amplitude, long-period returns to the starting diagonal elements in the density of states, have been shown in Sec. II F for a single-qubit Rabi model. Similar phenomena occur also in the two-qubit case. While for most

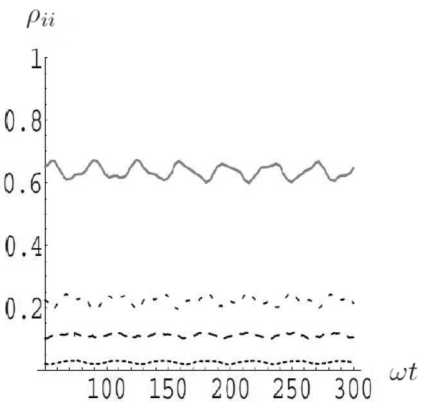

FIG. 10. Time-asymptotic diagonal density matrix elements under moderate spin-spin interaction ($\gamma' = 1$) in the Ising model coupling plotted against normalized time. Results are similar to those in Fig. 7, but with more noise. However, there is an *overall* decoherence as a result of the coupling. The diagonal matrix elements are, from top to bottom, for Uu,Lu,Ul,Ll. The parameter set is $[E = 5, e = 0.1, K = 4, k = 2.5, \omega = 1, \gamma = 0, \gamma' = -0.5]$.

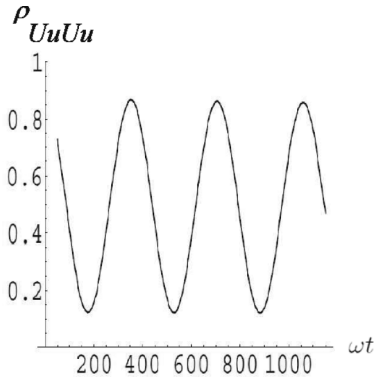

FIG. 11. Large-scale, large-period ($\gg 2\pi/\omega$) oscillations in the diagonal Uu component of the density matrix, superimposed on tiny, $\approx 2\pi/\omega$, oscillations (not visible). Parameter values are $[E=5, e=0.1, K=4, k=2.5, \omega=1, \gamma=0, \gamma'=-0.5]$.

values of the parameters the diagonal density matrix elements exhibit only small oscillations over the time range in the asymptotic, long-time range, typically, $\delta\rho \approx 1\%$, there are some singular values of the parameters where the oscillations are of the order of 100% and persist over several periods. The periods are in the range of $50 \times 2\pi/\omega$ or larger. An example of this behavior is shown in Fig. 11 for the parameter set $[E=5, e=0.1, K=4, \omega=1, k=2.5]$ at coupling strengths in the close vicinity of $\gamma'=-0.5$, but not at more than about 0.02 away from this value. Similar oscillations with comparable periods are observed for the parameter set $[E=5, e=0.1, K=2, k=1.25, \omega=1]$, near the coupling strength value of $\gamma'=0.8$.

The oscillations are even more remarkable in that the time period of $300/\omega$ does not have any simple physical explanation in terms of the parameter set. (This is unlike the revival time expression in [9], holding for weak coupling and the large $\langle N \rangle$ case.) Further investigation is needed to reveal the source of this result.

IV. DISCUSSION

In a two-qubit system whose energy splittings are (respectively) much larger and much smaller than the frequencies in externally induced time-dependent perturbations, the low-energy qubit decoheres, while the high-energy qubit maintains its purity, being adiabatically protected. While this may be intuitively obvious, we have also examined less obvious cases when the two qubits are coupled and have found that for large coupling strength the adiabatic protection wears off.

The time-averaging procedure used in here (introduced programmatically in Sec. II A) has been found to be, in practice, more time economic for achieving the density matrix truncation than the mainstream formalism of environment tracing. A more basic advantage is that, whereas in the latter method the truncation has to be enacted by some assumption of the nature and dynamics of the environment (e.g., the measuring apparatus, as in Sec. 1.1.2 in [24]), which is outside and beyond the Hamiltonian of the system itself, in the present formalism the same effect is achieved by the relatively simple manipulation (time averaging) of the *system's* Hamiltonians, such as those in Eqs. (1) and (9)–(12), without speculating on the time development of the environment. In this sense, then, the system's Hamiltonian is much more self-contained than that of the mainstream formalism. The choice of the time-dependent terms in the above equations is apparently *ad hoc* and arbitrary; we have also tried, in a preliminary way, other forms (such as a sum of oscillator terms, with random amplitudes and frequencies), and the results appear to be similar, except for the required time width for averaging. To present these results in a systematic form represents an extension of the present (single-frequency) model, which was named the "minimal model" in a recent presentation [36].

[1] M. Schlosshauer, Rev. Mod. Phys. **76**, 1267 (2005).
[2] R. Kubo, J. Math. Phys. **4**, 174 (1963).
[3] G. Gangopadhyay, M. S. Kumar, and S. Dattagupta, J. Phys. A: Math. Gen. **34**, 5485 (2001).
[4] D. Lidar and J. B. Whaley, in *Irreversible Quantum Dynamics*, Springer Lecture Notes in Physics, No. 622 (Springer Verlag, Berlin, 2003), pp. 83–120, also arXiv:quant-ph/0301032.
[5] A. Aharony, O. Entin-Wohlman, and S. Dattagupta, arXiv:0908.4385.
[6] A. Aharony, S. Gurvitz, Y. Tokura, O. Entin-Wohlman, and S. Dattagupta, arXiv:1205.5622.
[7] I. E. Farquhat, *Ergodic Theory in Statistical Mechanics* (Interscience, London, 1964), Chap. 2.
[8] I. I. Rabi, Phys. Rev. **49**, 324 (1936); **51**, 652 (1937).
[9] E. K. Irish, J. Gea-Banacloche, I. Martin, and K. C. Schwab, Phys. Rev. B **72**, 195410 (2005).
[10] S. Ashhab and F. Nori, Phys. Rev. A **81**, 042311 (2010).
[11] D. Braak, Phys. Rev. Lett. **107**, 100401 (2011).
[12] S. Agarwal, S. M. Hashemi Rafsanjani, and J. H. Eberly, arXiv:1201.2928.
[13] K. Ziegler, J. Phys. A: Math. Theor. **45**, 452001 (2012).
[14] D. Leibfried, R. Blatt, C. Monroe, and D. Wineland, Rev. Mod. Phys. **75**, 281 (2003).
[15] I. Thanopulos, E. Paspalakis, and Z. Kis, Chem. Phys. Lett. **390**, 228 (2004).
[16] A. T. Sornborger, A. N. Cleland, and M. R. Geller, Phys. Rev. A **70**, 052315 (2004).
[17] A. Wallraff *et al.*, Nature (London) **431**, 162 (2004); A. Wallraff, D. I. Schuster, A. Blais, L. Frunzio, J. Majer, M. H. Devoret, S. M. Girvin, and R. J. Schoelkopf, Phys. Rev. Lett. **95**, 060501 (2005).
[18] P. Forn-Diaz, J. Lisenfeld, D. Marcos, J. J. Garcia-Ripoll, E. Solano, C. J. P. M. Harmans, and J. E. Mooij, Phys. Rev. Lett. **105**, 237001 (2010).
[19] M. Steffen *et al.*, Science **313**, 1423 (2006).
[20] P. Yang, P. Zou, and Z.-M. Zhang, Phys. Lett. A **376**, 2977 (2012).
[21] J. H. von Neumann, *Mathematical Foundation of Quantum Mechanics* (Princeton University Press, Princeton, 1955), Chap. III.

[22] W. Band, *An Introduction to Quantum Statistics* (Van Nostrand, Princeton, 1955), Sec. 11.4.
[23] R. Englman and A. Yahalom, Phys. Rev. E **69**, 026120 (2004).
[24] A. E. Allahverdyan, R. Balian, and T. N. Niewenhuizen, arXiv:1107.2138v3 [quant-phys]; Phys. Rep. 00 (2013) 1-201.
[25] R. Gaspard and M. Nagaoka, J. Chem. Phys. **111**, 5668 (1999).
[26] W. H. Zurek, S. Habib, and J. P. Paz, Phys. Rev. Lett. **70**, 1187 (1993); W. H. Zurek, Prog. Theor. Phys. **89**, 281 (1993).
[27] J. P. Paz and W. H. Zurek, Phys. Rev. Lett. **82**, 5181 (1999).
[28] A. Leggett, S. Chakravarty, A. Dorsey, M. Fisher, A. Garg, and W. Zwerger, Rev. Mod. Phys. **59**, 1 (1987).
[29] R. Englman and A. Yahalom, Phys. Rev. B **69**, 224302 (2004).
[30] R. Rechtman and O. Penrose, J. Stat. Phys. **19**, 359 (1978).
[31] R. Englman, *The Jahn-Teller Effect in Molecules and Crystals* (Wiley, London, 1972), Sec. 3.
[32] M. V. Feigel'man, L. B. Ioffe, V. E. Kravtsov, and E. Cuevas, Ann. Phys. (NY) **325**, 1390 (2010); M. V. Feigel'man, L. B. Ioffe, and M. Mézard, Phys. Rev. B **82**, 184534 (2010).
[33] R. Biele and R. D'Agosto, J. Phys. Condens. Matter **24**, 273201 (2012).
[34] A. Daneri, A. Loinger, and G. M. Prosperi, Nucl. Phys. **33**, 297 (1962).
[35] A. Messiah, *Quantum Mechanics*, Vol. 2 (North Holland, Amsterdam, 1962), Chap. XVII, Sec. 11.
[36] R. Englman and A. Yahalom (unpublished).